Automated Classification of Myocardial Infarction Based on Auscultation Position Using Random Forest

Ira Puspasari*
*School of Electrical Engineering
and Informatics*
Institut Teknologi Bandung
Bandung, Indonesia
33221050@std.stei.itb.ac.id

Tati L. R. Mengko
*School of Electrical Engineering
and Informatics*
Institut Teknologi Bandung
Bandung, Indonesia
tati@stei.itb.ac.id

Agung W. Setiawan
*School of Electrical Engineering
and Informatics*
Institut Teknologi Bandung
Bandung, Indonesia
awsetiawan@stei.itb.ac.id

Trio Adiono
*School of Electrical Engineering
and Informatics*
Institut Teknologi Bandung
Bandung, Indonesia
tadiono@stei.itb.ac.id

Miftah Pramudyo
*Department of Cardiology
and Vascular*
Padjajaran University
Bandung, Indonesia
miftah.pramudyo@gmail.com

Abstract—**Myocardial Infarction is a disease requiring immediate treatment. ECG examination has the disadvantage of diagnosing MI signals. This research used phonocardiogram signals to classify myocardial infarction, specifically STEMI, and NSTEMI based on auscultation position. Signals were acquired from four auscultation positions: APEX, LLSB, LUSB, and RUSB for 30 seconds. The filtered signal is segmented each cycle using Shannon Energy (SE). The feature extraction obtains 12 time-frequency-statistic matrices from the segmented cycles. Normalized z-score used to evaluate all feature values. A random forest was applied to classify normal and abnormal signals. The findings indicated that the proposed approach has the best performance accuracy of 86%, precision of 84%, sensitivity of 85%, and F1 score of 84% at the LUSB (Pulmonary) position. This is in accordance with previous research observations that there was a pansystolic murmur in MI patients with optimal audibility at the LUSB. These findings can be used for reference examination of patients with pathological symptoms of MI. Our future research will improve the performance by focusing on features with low redundancy and essential information for each signal feature.**

Index Terms—**detection, myocardial infarction, phonocardiogram, auscultation**

I. INTRODUCTION

The second cause of death in Indonesia was an ischemic heart or cause of heart attack, with 95.68 cases. The mortality rate among individuals with Acute Myocardial Infarction (AMI) is approximately 30%, with half of these fatalities occurring before the patient arrives at the hospital [1]. MI based on electrocardiograph examination results can be divided into two, namely ST-Elevation Myocardial Infarction (STEMI) and Non-ST-Elevation Myocardial Infarction (NSTEMI) [2]. STEMI was characterized as a myocardial infarction (MI) displaying ST segment elevations in two adjacent ECG leads, with specific criteria varying based on the leads affected. In contrast, NSTEMI is described by ST depression or other ischemic ECG changes that did not fulfill the criteria for STEMI [3].

Another study applied a deep learning-based artificial intelligence (DLA) algorithm to detect MI, with specificity results of 83.0% and 89.4% [4]. ECG examination has the disadvantage that diagnosis of MI from ECG signal is more difficult when there is a left bundle branch block since it is similar to STEMI changes. The research investigated machine learning, including k-NN, SVM, Naive Bayes, and Random Forest-based automatic classification systems, utilizing heart sounds to diagnose cardiac disorders [5]. A previous study used Phonocardiogram (PCG) signals to classify the classification of normal and AWMI, IPWMI, and NSTEMI using MFCCs and Ensemble KNN with an accuracy value of 94.9%. However, this study did not describe the procedure for placing the stethoscope position on the pulmonary, aortic, mitral, and tricuspid valves [6]. Several important features to determine the difference between normal and MI signals include the time and energy features [7].

The Random Forest (RF) algorithm is a well-established and widely adopted supervised ensemble machine learning technique, primarily employed in real-time classification and related domains [8]. RF algorithm has robustness and high

prediction [9], [10]. Gosh et al. present a methodology for the automated identification of heart valve disorders, employing the RF algorithm. Their findings yielded accuracy (IA) rates of 98.83% for the normal class, 97.66% for AS, 91.16% for MS, and 92.83% for MR [11]. The time and frequency characteristics of heart sound signals were leveraged to construct utilizing the RF method. Notably, the accuracy achieved by this proposed algorithm surpassed the state-of-the-art approaches by approximately 12% [12]. PCG signal analysis was performed at various auscultation locations, such as the right upper sternal border (RUSB), left upper sternal border (LUSB), and left lower sternal border (LLSB). Previous research has differentiated normal and abnormal PCG signals using a convolutional neural network (CNN) with an accuracy of 86.8% [13]. However, there is no specific description of the auscultation position. Four hundred ninety-seven features will impact the computational complexity and time required for data analysis [14].

The ten essential features, the interquartile range, autocorrelation, mean absolute difference, zero crossing rate, entropy frequency, frequency, median frequency, spectral variation, spectral roll-off, and minimum, were used to differentiate the signals. Furthermore, this study will compare the APEX, LLSB, LUSB, and RUSB auscultation positions of normal and MI PCG signals.

II. RELATED WORK

Existing research has used four-auscultation position data in the auscultation process (recording heart sound signals using a digital stethoscope). It has been investigated by differentiating the signal at each position. The lowest value of sensitivity is found in the signal recorded at the mitral auscultation position, with a sensitivity of 71.2%, and specificity at the aortic auscultation position, with a value of 89.4% [15]. In a previous study, patients who exhibited a pathological systolic murmur with an intensity level exceeding two and were best heard at the LUSB, digital recordings obtained from that specific location and indicating possible pathology [16]. Detection of Acute Myocardial Infarction (AMI) using Deep Learning-Enabled Electrocardiograms, resulting in precision, sensitivity, specificity, and F1 values of the deep learning model for AMI diagnosis of 0.827, 0.824, 0.950, and 0.825 [1]. The method underwent testing on a dataset containing ECG records associated with MI. In summary, the method achieved remarkable performance metrics, including a sensitivity 92.4%, and specificity of 97.7% [17].

Many studies have developed MI classification using ECG signals recorded by applying deep learning and machine learning. However, few studies explain the classification of MI signals in PCG signal auscultation results. This study has explored PCG signals for Myocardial Infarction classification based on extracting PCG signals recorded on four auscultation positions. The extraction results are then classified using machine learning to obtain dominant features for MI classification.

TABLE I
CHARACTERISTIC OF THE SUBJECTS

Characteristics	Statistics
Normal subjects (year)	20-25
Abnormal subjects (year)	46-78
Female subject	7.5%
Male subject	92.5%
Normal Blood Pressure:	
Avg. Systolic (bpm)	121.5 ± 3.24
Avg. Diastolic (bpm)	80.2 ± 2.48
STEMI, NSTEMI Blood Pressure:	
Avg. Systolic (bpm)	112.8 ± 17.94
Avg. Diastolic (bpm)	73.9 ± 11.56
Therapies of Myocardial Infarction	no
(Cormobidities) No. Hypertension	11 (27.5%)
(Cormobidities) No. Diabetes mellitus	3 (7.5%)

III. PROPOSED METHOD

Fig.1. illustrates the sequential procedures, with a detailed description of the following steps. The following process used bandpass filtering on the normal signal to filter the 20-400 Hz [11]. The filtered signal has been segmented each cycle using Shannon Energy (SE) (1) [7]:

$$SE[k] = -x_{\hat{s}}[k]^2 log(x_{\hat{s}}[k])^2 \qquad (1)$$

In this study, there are three data classes, namely normal signals and MI signals, divided into STEMI and NSTEMI. Segmented signal data for Normal-APEX: 690 cycles, LLSB: 778 cycles, LUSB: 810 cycles, RUSB: 600 cycles. Number of segmented signal data for STEMI-APEX: 450 cycles, LLSB: 390 cycles, LUSB: 420 cycles, RUSB: 420 cycles. Number of segmented signal data for NSTEMI-APEX signals: 165 cycles, LLSB: 265 cycles, LUSB: 270 cycles, RUSB: 240 cycles.

A. PCG Signal Collection and Preprocessing

The PCG signals are collected at the Cardiac Center of Hadi Sadikin Hospital-Bandung Indonesia under ethical registration LB.02.01/X6.5/75/2022. The database contains 360 PCG recordings in audio (.wav). Table I shows the characteristics of the subject. The number of normal subjects is 30, and MI-stenosis is 60. The auscultation process uses a Littmann Cardiology IV electronic stethoscope. The sampling frequency (fs) is 8000 Hz.

B. Feature Extraction

As in previous studies, feature extractions were applied to classify PCG signals for normal and abnormal classification [18], [19].

- Time Domain: The autocorrelation (AR) feature can be defined as a function of the time lag between the initial signal and the delay signal (2) [20].

$$An(k) = \sum_{i=-\infty}^{\infty} x(i)z(j-i)x(i+k)z(j-k-i) \quad (2)$$

An(k) is the k-th autocorrelation "lag", x(i) is the heart sound signal, and z(j) is a window function. The negative turning points (NT) feature reduces the sampling rate
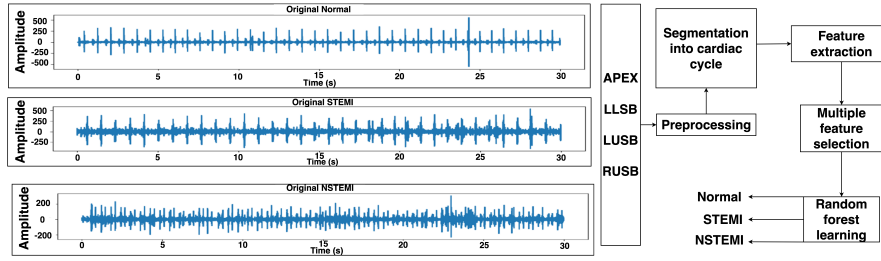
Fig. 1. Block diagram of the proposed method for MI classification

by half, selectively saving peaks and valleys (turning points) [21]. The mean absolute diff (MAD) is an average difference value that measures the absolute difference between the average amplitude values. ZCR (3) is the rate of sign change across the signal. Larger ZCR values are expected for abnormal signals [22]:

$$ZCR = 1/2 \sum_{i=2}^{n} |sign(a_i) - sign(a_{i-1})| \qquad (3)$$

- Frequency Domain: entropy based-features are calculated from finite values, or signal segments of PCG signals [23]. The frequency feature was calculated using Continuous Wavelet Transform (CWT). Fig.2. shows the normal and abnormal PCG scalograms. The scalogram provides the time-frequency characteristics by representing CWT (4). Mexican hat wavelet is appropriate for our study.

$$CWT_M(i,j) = \int_{-\infty}^{\infty} x(t)\psi_{i,j}(t) \qquad (4)$$

However, based on each class's auscultation position, there is no visible difference. Therefore, it is essential to explore the data of each auscultation position further. Consequently, some time domain features are needed to differentiate more detailed characteristics, including spectral distance (SD), median frequency (MF), spectral variation (SV), and spectral roll-off (SRO). SD is a measure to calculate the distance between the maximum magnitudes. MF is used to obtain the center value of the frequency spectrum. A measure of SV was applied in this study to see the diversity of spectral values in normal and MI signals. SRO (5) is defined as the Kth percentile (85% or 95%) of the cumulative power spectral distribution within the PCG signal [5].

$$\sum_{i=1}^{Roll-off} A_t[i] = 85 \qquad (5)$$

At [i] is the frequency component value at the i-th frequency bin and frame t.

- Statistical Domain: the interquartile range (IR) is a measure of statistical dispersion, which is the spread of the data [24].

C. Classification

All feature values have been evaluated using the normalized z-score [25]. After evaluating the feature values from the matrix of each PCG cycle, the 12-dimensional value vector of the features was further evaluated using a classifier. This study used the RF Classifier. The value of the RF classifier evaluation metric will be significantly influenced by several vital parameters, including the number of splits, trees, tree depth, and random state [11], [26]. This research has applied 200 random state and overall accuracy (OA) values to evaluate the performance of the RF classifier. The tenfold cross-validation methods are applied for selecting the training and test PCG cycle instances of RF [27].

IV. RESULT AND DISCUSSION

Several comparison feature combination evaluations have different accuracy values, as shown in Table II. This study has evaluated 12 features with eight multi-feature combination models at each auscultation position. The test results found that the application of three features, namely minimum value, frequency, and SRO, had the lowest accuracy value of 58.3% on the RUSB, 59.2% on the LLSB, 61.6% on the APEX, and 65.7% on the LUSB. Tests have been conducted using 12 features in this research, and there is an increase in accuracy of 21.2% on the APEX, 19.2% on the LLSB, 19% on the LUSB, and 20.3% on the RUSB. Each feature model has been evaluated at each auscultation position, and the highest accuracy results for all feature models are found on the LUSB. The highest accuracy value has been obtained by 86% using ten multiple features named model 7. Fig. 3 shows a comparison of the average accuracy at each auscultation position with eight feature combination models for MI signal classification. Thompson et al. presented a classification system wherein pansystolic murmurs of intensity grade exceeding three, localized at LUSB [16].

These six discerning signs encompassed the following characteristics: a murmur of intensity grade of more than 3, optimal audibility at the LUSB, a harsh quality, a pansystolic timing pattern, the presence of a systolic click, or the existence of an abnormal second heart sound [31]. An ECG was employed to ascertain the presence of an acute STEMI situated anteriorly, and a novel pansystolic murmur was detected [32]. The RF classifier performance for cross-validation is shown in Table III. It is observed that the RF classifier has the highest accuracy
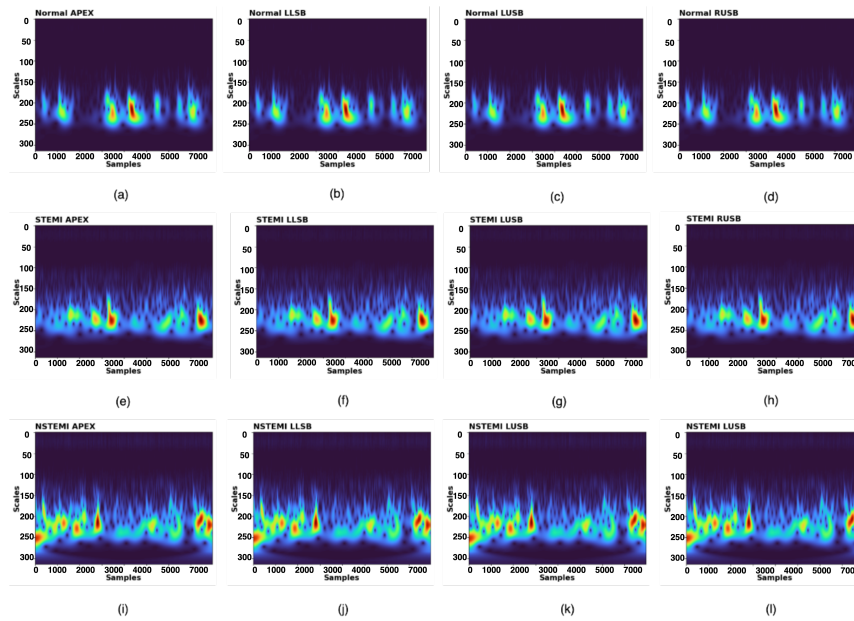
Fig. 2. PCG Scalogram (a) Normal-APEX, (b) Normal-LLSB, (c) Normal-LUSB, (d) Normal-RUSB, (e) STEMI-APEX, (f) STEMI-LLSB, (g) STEMI-LUSB, (h) STEMI-RUSB, (i) NSTEMI-APEX, (j) NSTEMI-LLSB, (k) NSTEMI-LUSB, (l) NSTEMI-RUSB.

TABLE II
PERFORMACE EVALUATION BASED ON MULTIPLE FEATURES COMBINATION

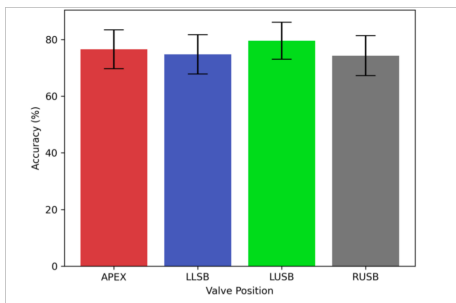| Model	Multiple Features												Accuracy (%)			
	IR	Min	AC	NT	MAD	ZCR	EF	Freq	SD	MF	SV	SRO	APEX	LLSB	LUSB	RUSB
1								v				v	61.6	59.2	65.7	58.3
2		v				v			v		v		73.6	72.1	75.3	71.8
3	v		v		v		v			v			79.3	75.6	80.0	77.8
4		v		v		v		v	v		v	v	77.8	76.3	83.0	80.2
5	v			v	v		v		v	v	v	v	81.6	82.6	82.7	79.0
6		v	v			v		v	v	v	v		75.1	78.0	79.7	74.6
7	v	v	v		v	v	v	v		v	v	v	81.2	76.3	**8**6.0	74.6
8	v	v	v	v	v	v	v	v	v	v	v	v	82.8	78.4	84.7	78.6

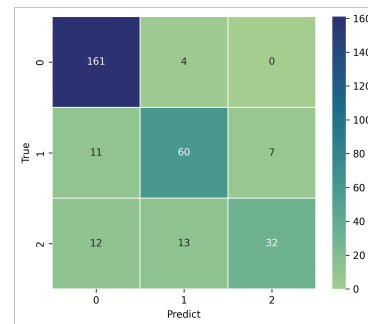Fig. 3. The performance of RF based on auscultation position

Fig. 4. Confusion matrix testing RF

value on LUSB, which was 85.2%. Fig. 4. shows the confusion matrix testing on RF using model 7.

Previous research has established that CAD is associated with the production of murmurs [19]. Table IV. shows the comparative study of PCG signal classification. The binary classification employs an ANN classifier. An accuracy level of 82.57% is achieved when combining the signals acquired from the tricuspid, mitral, and midaxillary regions [28]. In a previous study with 94.9% accuracy for MI signal classification using a KNN ensemble, the auscultation position was not

TABLE III
PERFORMACE EVALUATION BASED ON MULTIPLE FEATURES COMBINATION

Cross valida-tion 10-fold	Model 1 (%)	Model 2 (%)	Model 3 (%)	Model 4 (%)	Model 5 (%)	Model 6 (%)	Model 7 (%)	Model 8 (%)
APEX	65.3 ± 3.4	76. 5 ± 3.4	75.6 ± 2.5	78.4 ± 3.4	80.8 ± 4.1	79.3 ± 2.6	81.9 ± 2.5	83.3 ± 4.0
LLSB	64.1 ± 3.4	73.9 ± 3.5	71.6 ± 2.6	76.2 ± 3.4	77.8 ± 3.6	76.9 ± 3.0	80.9 ± 3.8	81.1 ± 3.3
LUSB	60.9 ± 2.7	85.2 ± 2.1	74.5 ± 3.5	78.9 ± 2.4	81.2 ± 2.3	80.2 ± 2.5	81.4 ± 2.4	82.5 ± 2.2
RUSB	59.2 ± 2.1	79.7 ± 4.3	48.4 ± 4.7	76.4 ± 2.0	80.9 ± 3.2	77.6 ± 4.7	81.6 ± 3.1	83.0 ± 4.4

TABLE IV
COMPARATIVE STUDY OF PCG SIGNAL CLASSIFICATION

Reference, year	Feature	Auscultation position	Classifier	Performance (%)
[19], 2015	Spectrum	no	QDA	Sen = 72.00%, Spec = 65.20%
[28], 2019	Time-Freq domain	yes	ANN	Acc = 82.57%, Sen = 85.61%, Spec = 79.55%
[29], 2019	MFCC	no	RNN+LSTM	Acc = 80.80%
[6], 2020	MFCC	no	Ensemble Subspace KNN	Acc = 94.9%
[13], 2020	497 features	no	CNN	Acc = 86.8%, Sen = 87%, Spec = 86.6%
[30], 2020	CWT, SST, Entropy	yes	SSVM, KNN	Acc = 81.92%, Sen = 82.79%, Spec = 81.04%
[15], 2021	no	yes	ResNet	Sen = 76.3%, Spec = 91.4%
Proposed Method	**10 features**	**yes**	**Random Forest**	**Acc = 86%, Prec = 84%, Sen = 85%, F1 Score = 84%**

detailed yet, and the highest accuracy for each auscultation position was discussed [6]. Chorba et al. detected clinically significant murmurs and valvular heart disease. The highest sensitivity value was found in the signal at the Pulmonic auscultation position at 81.9% [15]. Existing research on murmurs in CAD examining the position of each valve using KNN and SVM classification gives the results of the Acc of 81.92% [30]. The absolute reduction in mortality was most significant among patients who presented within one hour of symptom onset (average delay 0.75 h) [33]. If the patient's symptoms lead to MI, further examination uses an ECG, which takes 5-10 minutes, then waits for the results of the cardiologist's reading. Conversely, failure to address this issue frequently leads to suboptimal medical procedure results and increased mortality rates [34]. Furthermore, the troponin test was applied, and the blood samples should be collected at least 6-9 hours following the onset of symptoms to determine cardiac troponin concentrations before making a definitive diagnosis [35]. The time required using the proposed method in this study is 3 minutes 56 seconds. MI has a golden hour condition where the heart muscle begins to die within 80-90 minutes after the blood supply is cut off [7]. This study provides a classification system based on the position of the auscultation examination; thereby, it can reduce diagnosis time to treat patients quickly and adequately, prevent increased heart muscle death, and, hence, reduce mortality rates.

Finally, we identified ten essential features in building ML models to differentiate MI with an Acc: 86%, Prec: 84%, and Sen: 85%. This research has produced a False Negative Rate (FNR) value of 0.11. FNR's score can substantially affect patients' well-being in the medical field. A high FNR result may fail to detect many cases [36]. Previous research has produced FNR values on time domain features of 0.33, a frequency domain of 0.25, and a time-frequency of 0.16 [37]. These findings suggest the potential for simplified identification of MI-stenosis monitoring systems to reduce hospitalization rates.

V. CONCLUSION

A method based on the evaluation of feature extraction in the time, frequency, and statistical domain of the PCG signal has been introduced to classify STEMI and NSTEMI pathologies on four auscultation positions. Twelve features have been used and validated, including autocorrelation, negative turning points, mean absolute diff, ZCR, entropy frequency, frequency, spectral distance, median frequency, spectral variation, spectral roll-off, IQR, and minimum. The RF classifier has been used to classify normal and MI signals. The classification performance based on the proposed method results in an Acc: 86%, Prec: 84%, Sen: 85%, and F1-Score: 84% at the LUSB auscultation position. Future research explores different types of features and automatic feature selection methods to improve classifier performance.

REFERENCES

[1] X. Chen, W. Guo, L. Zhao, W. Huang, L. Wang, A. Sun, L. Li, and F. Mo, "Acute myocardial infarction detection using deep learning-enabled electrocardiograms," *Frontiers in cardiovascular medicine*, vol. 8, p. 654515, 2021.

[2] J. Kingma *et al.*, "Myocardial infarction: An overview of stemi and nstemi physiopathology and treatment," *World Journal of Cardiovascular Diseases*, vol. 8, no. 11, p. 498, 2018.

[3] M. Saleh and J. A. Ambrose, "Understanding myocardial infarction," *F1000Research*, vol. 7, 2018.

[4] Y. Cho, J.-m. Kwon, K.-H. Kim, J. R. Medina-Inojosa, K.-H. Jeon, S. Cho, S. Y. Lee, J. Park, and B.-H. Oh, "Artificial intelligence algorithm for detecting myocardial infarction using six-lead electrocardiography," *Scientific reports*, vol. 10, no. 1, p. 20495, 2020.

[5] A. Yadav, A. Singh, M. K. Dutta, and C. M. Travieso, "Machine learning-based classification of cardiac diseases from pcg recorded heart sounds," *Neural Computing and Applications*, vol. 32, pp. 17843–17856, 2020.

[6] M. U. Khan, Z. Mushtaq, M. Shakeel, S. Aziz, and S. Z. H. Naqvi, "Classification of myocardial infarction using mfcc and ensemble subspace knn," in *2020 international conference on electrical, communication, and computer engineering (ICECCE)*. IEEE, 2020, pp. 1–5.

[7] I. Puspasari, T. L. Mengko, A. W. Setiawan, T. Adiono, and M. Pramudyo, "Denoising of heart sound signal for myocardial infarction detection based on adaptive filtering," in *2023 IEEE 5th Eurasia Conference on Biomedical Engineering, Healthcare and Sustainability (ECBIOS)*. IEEE, 2023, pp. 213–216.

[8] T. S. Roy, J. K. Roy, and N. Mandal, "Classifier identification using deep learning and machine learning algorithms for the detection of valvular heart diseases," *Biomedical Engineering Advances*, vol. 3, p. 100035, 2022.

[9] J. Oliveira, D. Nogueira, C. Ferreira, A. M. Jorge, and M. Coimbra, "The robustness of random forest and support vector machine algorithms to a faulty heart sound segmentation," in *2022 44th Annual International Conference of the IEEE Engineering in Medicine & Biology Society (EMBC)*. IEEE, 2022, pp. 1989–1992.

[10] R. Gonzalez-Landaeta, B. Ramirez, and J. Mejia, "Estimation of systolic blood pressure by random forest using heart sounds and a ballistocardiogram," *Scientific Reports*, vol. 12, no. 1, p. 17196, 2022.

[11] S. K. Ghosh, R. K. Tripathy, R. Ponnalagu, and R. B. Pachori, "Automated detection of heart valve disorders from the pcg signal using time-frequency magnitude and phase features," *IEEE Sensors Letters*, vol. 3, no. 12, pp. 1–4, 2019.

[12] M. Nassralla, Z. El Zein, and H. Hajj, "Classification of normal and abnormal heart sounds," in *2017 Fourth International Conference on Advances in Biomedical Engineering (ICABME)*. IEEE, 2017, pp. 1–4.

[13] F. Li, H. Tang, S. Shang, K. Mathiak, and F. Cong, "Classification of heart sounds using convolutional neural network," *Applied Sciences*, vol. 10, no. 11, p. 3956, 2020.

[14] D. Stiawan, M. Y. B. Idris, A. M. Bamhdi, R. Budiarto *et al.*, "Cicids-2017 dataset feature analysis with information gain for anomaly detection," *IEEE Access*, vol. 8, pp. 132911–132921, 2020.

[15] J. S. Chorba, A. M. Shapiro, L. Le, J. Maidens, J. Prince, S. Pham, M. M. Kanzawa, D. N. Barbosa, C. Currie, C. Brooks *et al.*, "Deep learning algorithm for automated cardiac murmur detection via a digital stethoscope platform," *Journal of the American Heart Association*, vol. 10, no. 9, p. e019905, 2021.

[16] W. Thompson, C. Hayek, C. Tuchinda, J. Telford, and J. Lombardo, "Automated cardiac auscultation for detection of pathologic heart murmurs," *Pediatric cardiology*, vol. 22, pp. 373–379, 2001.

[17] H. W. Lui and K. L. Chow, "Multiclass classification of myocardial infarction with convolutional and recurrent neural networks for portable ecg devices," *Informatics in Medicine Unlocked*, vol. 13, pp. 26–33, 2018.

[18] Y. Chen, S. Wang, C.-H. Shen, and F. K. Choy, "Matrix decomposition based feature extraction for murmur classification," *Medical engineering & physics*, vol. 34, no. 6, pp. 756–761, 2012.

[19] S. E. Schmidt, C. Holst-Hansen, J. Hansen, E. Toft, and J. J. Struijk, "Acoustic features for the identification of coronary artery disease," *IEEE Transactions on Biomedical Engineering*, vol. 62, no. 11, pp. 2611–2619, 2015.

[20] C.-H. Wu, C.-W. Lo, and J.-F. Wang, "Computer-aided analysis and classification of heart sounds based on neural networks and time analysis," in *1995 International Conference on Acoustics, Speech, and Signal Processing*, vol. 5. IEEE, 1995, pp. 3455–3458.

[21] A. López, F. J. Ferrero, and J. R. Villar, "Eog signal compression using turning point algorithm," in *2021 IEEE International Instrumentation and Measurement Technology Conference (I2MTC)*. IEEE, 2021, pp. 1–4.

[22] M. Singh and A. Cheema, "Heart sounds classification using feature extraction of phonocardiography signal," *International Journal of Computer Applications*, vol. 77, no. 4, 2013.

[23] A. Ganguly and M. Sharma, "Detection of pathological heart murmurs by feature extraction of phonocardiogram signals," *Journal of Applied and Advanced Research*, vol. 2, no. 4, pp. 200–205, 2017.

[24] S. J. Reinstadler, T. Stiermaier, C. Eitel, G. Fuernau, M. Saad, J. Pöss, S. De Waha, M. Mende, S. Desch, B. Metzler *et al.*, "Impact of atrial fibrillation during st-segment–elevation myocardial infarction on infarct characteristics and prognosis," *Circulation: Cardiovascular Imaging*, vol. 11, no. 2, p. e006955, 2018.

[25] H. Wen and J. Kang, "Searching for effective neural network architectures for heart murmur detection from phonocardiogram," in *2022 Computing in Cardiology (CinC)*, vol. 498. IEEE, 2022, pp. 1–4.

[26] P. Dutta, S. Paul, K. Cengiz, R. Anand, and M. Majumder, "A predictive method for emotional sentiment analysis by machine learning from electroencephalography of brainwave data," in *Implementation of Smart Healthcare Systems using AI, IoT, and Blockchain*. Elsevier, 2023, pp. 109–130.

[27] R. Tripathy, L. Sharma, and S. Dandapat, "Detection of shockable ventricular arrhythmia using variational mode decomposition," *Journal of medical systems*, vol. 40, pp. 1–13, 2016.

[28] P. Samanta, A. Pathak, K. Mandana, and G. Saha, "Classification of coronary artery diseased and normal subjects using multi-channel phonocardiogram signal," *Biocybernetics and Biomedical Engineering*, vol. 39, no. 2, pp. 426–443, 2019.

[29] A. Raza, A. Mehmood, S. Ullah, M. Ahmad, G. S. Choi, and B.-W. On, "Heartbeat sound signal classification using deep learning," *Sensors*, vol. 19, no. 21, p. 4819, 2019.

[30] A. Pathak, P. Samanta, K. Mandana, and G. Saha, "Detection of coronary artery atherosclerotic disease using novel features from synchrosqueezing transform of phonocardiogram," *Biomedical Signal Processing and Control*, vol. 62, p. 102055, 2020.

[31] K. M. Smith, "The innocent heart murmur in children," *Journal of Pediatric Health Care*, vol. 11, no. 5, pp. 207–214, 1997.

[32] E. Flores-Umanzor, G. Caldentey, and R. San Antonio, "New holosystolic murmur after acute myocardial infarction," *European Heart Journal: Acute Cardiovascular Care*, vol. 9, no. 5, pp. NP5–NP6, 2020.

[33] E. Boersma, A. C. Maas, J. W. Deckers, and M. L. Simoons, "Early thrombolytic treatment in acute myocardial infarction: reappraisal of the golden hour," *The Lancet*, vol. 348, no. 9030, pp. 771–775, 1996.

[34] H. M. Ahn, H. Kim, K. S. Lee, J. H. Lee, H. S. Jeong, S. H. Chang, K. R. Lee, S. H. Kim, and E. Y. Shin, "Hospital arrival rate within golden time and factors influencing prehospital delays among patients with acute myocardial infarction," *Journal of Korean Academy of Nursing*, vol. 46, no. 6, pp. 804–812, 2016.

[35] F. S. Apple and A. H. Wu, "Myocardial infarction redefined: role of cardiac troponin testing," pp. 377–379, 2001.

[36] M. Hassanuzzaman, N. A. Hasan, M. A. Al Mamun, M. Alkhodari, K. I. Ahmed, A. H. Khandoker, and R. Mostafa, "Recognition of pediatric congenital heart diseases by using phonocardiogram signals and transformer-based neural networks," in *2023 45th Annual International Conference of the IEEE Engineering in Medicine & Biology Society (EMBC)*. IEEE, 2023.

[37] M. Milani, P. E. Abas, L. C. De Silva, and N. D. Nanayakkara, "Abnormal heart sound classification using phonocardiography signals," *Smart Health*, vol. 21, p. 100194, 2021.